



Experimental Investigation Of Flow Dynamics Effects Of Cooling With A Circular Impinging Jet

Nevin ÇELİK^{1*}, Celal KISTAK², Haydar EREN³

¹ Firat University, Mechanical Engineering Department, nevincelik@firat.edu.tr, Orcid No: 0000-0003-2456-5316

² Firat University, Mechanical Engineering Department, ckistak@firat.edu.tr, Orcid No: 0000-0003-4621-5405

³ Firat University, Mechanical Engineering Department, haydar@firat.edu.tr, Orcid No: 0009-0008-5097-5080

ARTICLE INFO

Article history:

Received 7 January 2025

Received in revised form 22 March 2025

Accepted 25 March 2025

Available online 30 June 2025

Keywords:

Impinging jets, Heat Transfer,
Turbulent intensity

ABSTRACT

This study experimentally investigates the effects of a circular impinging jet on heat transfer and flow dynamics. Using an aluminum nozzle with a diameter of $d=13.8$ mm, experiments were conducted within the Reynolds number range of 5000–25000. The nozzle-to-plate distance (h/d) was varied between $h/d=2-10$ to evaluate the jet's performance. Local Nusselt numbers (Nu), stagnation point Nusselt number (Nu_0), and average Nusselt numbers (Nu_{avg}) were analyzed in detail. The results demonstrated that both the nozzle-to-plate distance and Reynolds (Re) number significantly influence heat transfer performance. Increased Reynolds numbers and optimal h/d distances led to enhanced heat transfer at the stagnation point. These findings highlight the potential of impinging jets for energy-efficient cooling applications. The optimal nozzle-to-plate distance for maximum heat transfer was found to be $h/d = 6$, with a 30.5% increase in Nusselt number at $Re = 25000$. Additionally, turbulence intensity played a crucial role in heat transfer performance, particularly in the wall jet region, where it enhanced mixing and improved thermal efficiency.

DOI: 10.24012/dumf.1614964

* Corresponding author

Introduction

Impinging jets are widely used methods in engineering and industry to meet high heat transfer and energy efficiency requirements. When the fluid leaves the nozzle and comes into contact with a surface, a thin thermal boundary layer is formed, especially in the region of stagnation. This increases the momentum effect of the fluid and leads to a significant increase in both heat and mass transfer rates. The earlier study by Jambunathan et al. [1] revealed that the Nusselt number at stagnation in the laminar regime is proportional to the square root of the centreline velocity this finding emphasised the strong connection between heat transfer and flow dynamics. Gordon and Akfirat [2] studied the turbulence characteristics of slot jets and analysed the effect of turbulence on heat transfer in detail, while Schlunder and Gnielinski [3] showed that maximum heat transfer is obtained when the nozzle-plate distance h/d is 7.5.

In recent years, studies on geometrical arrangements, pulsation characteristics and flow parameters of impinging jets have provided extensive results to improve system performance. The study of Kistak et al. [4] revealed that Reynolds number is the most effective parameter on heat transfer and this effect has a contribution rate of 82%.

Another study by Taskiran et al. [5] emphasised that double pulsative jets increase the local Nusselt number due to vortex formation and nanoparticle concentration further improves the performance. In the study of Bai and Gong [6], it was reported that the increase in surface velocity as a result of the interaction of moving surfaces and jet flow provides a significant improvement in heat transfer rates. In studies examining the effects of surface geometry and flow parameters, the importance of nanotechnology and pulsative flow combinations has been emphasised. Celik and Eren [7] investigated turbulent flow conditions in coaxial jets and emphasised the critical role of jet geometry in heat transfer performance. Baghel et al. [8] evaluated the contribution of surface velocity and jet momentum to heat transfer in liquid jets impinging on moving surfaces. Rahimi and Soran [9] investigated the effects of slot jets on moving surfaces and showed that surface velocity positively affects flow dynamics and heat transfer properties. In Wang and Elmi's study [10], it was stated that the distance between jets should be optimised in terms of energy transport and that $h/d = 6 - 8$ is ideal.

In this study, experimental studies using a circular pipe jet geometry ($d = 13.8$ mm) were taken as a basis and the effect of the impinging jet on heat transfer under turbulent flow conditions was investigated in detail. Such studies provide

important contributions to the development of energy efficient cooling systems and industrial applications.

Material And Methods

Experimental Setup

The experimental setup utilised in this study is depicted schematically in Figure 1. The jet flow was facilitated by a 500-litre capacity compressor, capable of storing compressed air up to a maximum pressure of 12 bar. The compressor was supported by a pressure gauge, an outlet valve, and an air conditioner. The air conditioner ensured that the compressed air was free from contaminants such as moisture, dust and particles, and the air flow was sent to the rotameters at the desired pressure with the help of the pressure regulator on it. During the experiment, the jet outlet flow rate was measured by two different rotameters with a measurement range of 0-20 m^3/h and 10-100 m^3/h in order to provide precise measurement. The jet system was supplied through a flat circular pipe, composed of aluminium and characterised by a smooth and seamless surface. From the rotameter outlet, a 2 m long straight hose was connected to the nozzle. The length of the nozzle was set at 32d to ensure fully developed flow conditions in a circular cross-section pipe flow.

The impingement plate was manufactured from 0.5 mm thick Cr-Ni stainless steel sheet and designed as a 53 cm wide, 59 cm high, 2.5 cm thick vertical channel. The front surface of the impingement plate was operated under constant temperature conditions to be used for the experiments. Constant temperature conditions were achieved by directing saturated water vapour from a steam boiler into the channel from bottom to top. By this method, a constant temperature of 96 °C was measured at the impingement surface of the duct. The vapour passing through the impingement surface was discharged to the external environment through a chimney located at the top of the duct. In order to minimise heat losses, the side and rear surfaces of the duct were insulated with a suitable insulation material. This experimental setup was designed and optimised to precisely evaluate the effects of jet impingement on flow and heat transfer. Temperature and velocity measurements were recorded with a CAMPBELL CR10X model data acquisition device connected to a personal computer. For velocity measurements, three separate velocity probes with a measurement range of 0.125-50 and 0.05-2.5 m/s were used.

Data Reduction and Uncertainty Analysis

Temperature measurements were made under conditions where the experiment was carried out in the continuous regime. During the jet impingement, temperature measurements were carried out on the back surface of the duct in contact with the vapour, since the thermocouples placed on the impingement surface are likely to disturb the flow dynamics. However, in order to evaluate the accuracy of this method, a series of preliminary experiments were carried out to analyse the effect of conduction heat transfer through the thickness of the plate on the measurement results.

In the preliminary tests, temperature measurements were carried out on the front surface (impingement surface) and the back surface of the duct before the jet was impinged, with the steam boiler in operation. Based on these measurements, the conduction heat transfer through the thickness of the plate was quantitatively calculated. The results revealed that the heat transfer by conduction is only 0.5% of the total heat transfer. This indicates that the effect of conduction heat transfer through the thickness of the plate on the experimental results is negligible.

In the light of these findings, it was accepted that the fact that the experimental temperature measurements were based on measurements made on the back surface of the plate would not affect the accuracy of the results obtained. Therefore, all temperature measurements were conducted on the basis of data obtained from the rear surface. This method was selected in order to enhance the reliability of the measurements and to circumvent any potential distortion of the flow dynamics.

$$h_{condens} = 0.943 \frac{[g\rho_L(\rho_L - \rho_v)kL^3 h_{fg}]^{1/4}}{\mu_L(T_{sat} - T_s)L} \quad (1)$$

Here, the expression h_{fg}' in terms of Jakob number developed by Rohsenow is used instead of latent heat of vaporisation (h_{fg}) :

$$h_{fg}' = h_{fg}(1 + 0.68Ja) \quad (2)$$

$$Ja = Cp_L \frac{\Delta T}{h_{fg}} = Cp_L \frac{(T_{sat} - T_s)}{h_{fg}} \quad (3)$$

Jacob (Ja) number is a dimensionless number used in condensation heat transfer. In the terms in Eq. (1)-(3), the sub-index v indicates the properties of vapour. The thermo-physical properties in Eq. (1) are chosen to depend on the bulk temperature (T_b) (but the latent heat of vaporisation h_{fg} and the vapour density are chosen to depend on the saturation temperature (T_{sat})). Thus, the total heat is found: The validity of the Eq. (1) used to calculate the heat transfer in condensation has been examined by scientists.

$$Q_{condens} = h_{condens}A(T_{sat} - T_s) \quad (4)$$

A more detailed boundary layer analysis based on Eq. (1) for film condensation on a vertical plate was carried out by Sparrow and Gregg [11]. This result, later confirmed by Chen [12], shows that the errors arising from the use of Eq. (1) are less than 3% for $Ja \leq 0.1$ and $1 \leq Pr \leq 100$. The agreement of the empirical Eq. (1) with the experimental data was also tested in this study, and it was observed that the agreement with the experimental results was about $\pm 4.3\%$ [13]. The amount of heat generated by condensation is the total amount of heat in the system. When the heat lost by natural convection and radiation is subtracted from the total heat, the remaining value is the net heat amount. The amount of heat by natural convection is obtained with the help of the empirical relation [14].

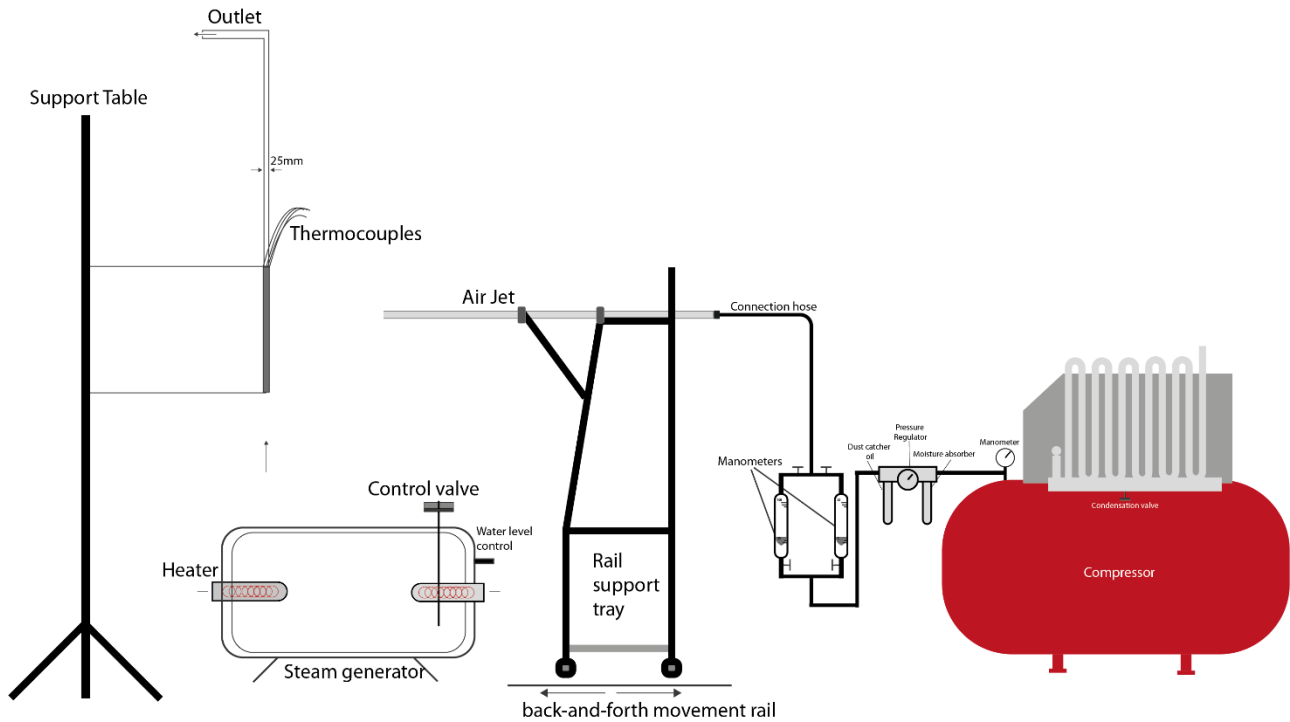


Fig. 1 Schematic representation of the experimental setup

The quantity of heat generated by condensation is equivalent to the total heat content of the system. Upon subtraction of the heat lost through natural convection and radiation from the total heat, the residual value constitutes the net heat amount. The heat transferred through natural convection can be calculated using the empirical relation [14].

$$Nu_{nat} = 0.68 + \left[\frac{0.67 Ra_l^{1/4}}{[1 + (0.492/Pr)^{9/16}]^{4/9}} \right] \quad (5)$$

$$Nu = \frac{h_{nat} L}{k_{air}} \quad (6)$$

$$Q_{nat} = h_{nat} A (T_s - T_{\infty}) \quad (7)$$

The amount of heat lost by radiation is:

$$Q_{rad} = \varepsilon \sigma A (T_s^4 - T_{\infty}^4) \quad (8)$$

Thus, net heat and then convection heat transfer coefficient is found:

$$Q_{net} = Q_{condens} - (Q_{nat} - Q_{rad}) \quad (9)$$

$$Q_{net} = Q_{conv} = h_{local} A (T_w - T_j) \quad (10)$$

$$h_{local} = \frac{Q_{net}}{A(T_w - T_j)} \quad (11)$$

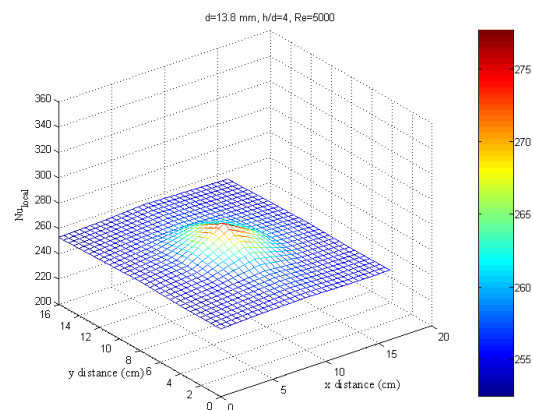
$$Nu = \frac{h_{local} d}{k} \quad (12)$$

In this study, temperature, velocity and flow rate measurements were made and Nusselt number, Reynolds number and turbulence intensity were calculated with the values obtained from these measurements. The uncertainty of the calculated values was carried out using the method developed by Kline and McClintock [15] with 95%

reliability. Accordingly, the highest uncertainty calculated for Nusselt number is $\pm 4.97\%$, for Reynolds number $\pm 2.89\%$ and for turbulence intensity $\pm 2.84\%$.

RESULTS AND DISCUSSIONS

In this study, where circular nozzles are used, the convective heat transfer between the hot plate and the jet flow is evaluated by the Nusselt number (Nu), which is a dimensionless expression. The dimensionless distance between the nozzle and the plate was set as $h/d = 4$ and the experiments were carried out for values of the Reynolds number between $Re = 5000$ and 25000 . The locally calculated the Nusselt number (Nu) and the average Nusselt numbers (Nu_{avg}) calculated at the geometrical centre point (Nu_0) of the plate are presented graphically based on the data obtained. In the experiments, measurement and data logging were carried out with a data logger with limited temperature measurement input.


 Fig. 2 Local Nu number distribution for $d=13.8$ mm, $h/d=4$, $Re=5000$

This limitation precluded the possibility of taking temperature measurements at very close intervals on the plate. However, intermediate values were calculated using computer-aided interpolation methods, thus enabling the local Nusselt distribution to be presented in more detail on the plate surface. The resulting graphs facilitated a more understandable representation of the local Nusselt distribution and made a significant contribution to the visualisation of the experimental results. In Figs. 2-5 local Nusselt distributions are given. The highest Nu number on the nozzle occurred at the stagnation point in all experiments. Increasing the Re number increased the stagnation point Nusselt number (Nu_0) Increased Reynolds numbers and optimal h/d distances led to enhanced heat transfer at the stagnation point significantly. However, while increasing the Reynolds number enhances heat transfer, it also introduces certain drawbacks. At higher Reynolds numbers, turbulence intensity increases significantly, leading to flow instability and uneven cooling distribution on the surface. This can result in localized overheating or inefficiencies in heat transfer. Additionally, higher jet velocities require greater energy input, leading to increased power consumption, which may not be ideal for energy-efficient applications. Another critical issue is the potential for surface erosion caused by the high-speed impinging jet, which may degrade material integrity over time. Therefore, selecting an optimal Reynolds number is crucial to balancing heat transfer performance, energy efficiency, and surface durability. While $Nu_0=277.5$ at $Re = 5000$, it increased to $Nu_0= 300.2$ with an increase of 8.1% compared to $Re = 5000$ when $Re=10000$. Likewise, when the number of Re was increased to 15000, $Nu_0= 320.9$ with an increase of 15.6% compared to $Re = 5000$, $Nu_0= 343.1$ with an increase of 23.5% at $Re = 20000$ and finally $Nu_0 = 362.5$ with an increase of 30.5% at $Re = 25000$. The distance between the nozzle and the slab undoubtedly has an effect on these high ratios.

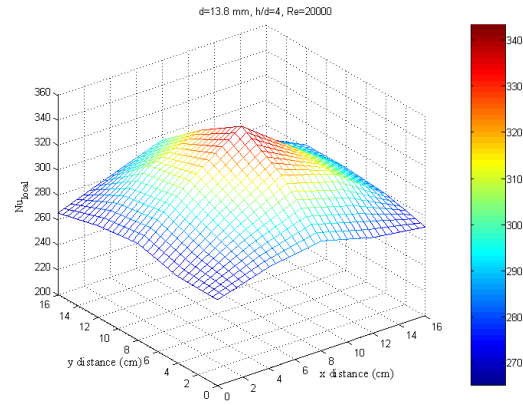


Fig. 4 Local Nu number distribution for $d = 13.8$ mm, $h/d = 4$, $Re = 20000$

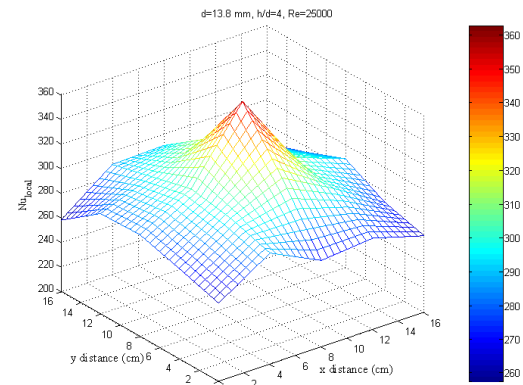


Fig. 5 Local Nu number distribution for $d = 13.8$ mm, $h/d = 4$, $Re = 25000$

Another striking point in the graphs is that the local Nu numbers increase on the surface from the stagnation point (in radial direction) with increasing Re number. When the Re number is 5000, a decrease of 8.69% is observed between the Nusselt number calculated at the stagnation point Nusselt number measured at the farthest point from the stagnation point In other words, the local Nu numbers are distributed with a difference of 8.69% from the centre point to the farthest point on the plate. Increasing the Re number has increased this decrease even more. Namely: 15.11% at $Re=10000$, 17.77% at $Re=15000$, 21.63% at $Re=20000$ and finally 27.32% at $Re=25000$. In Fig. 6 variation of stagnation point with Re given.

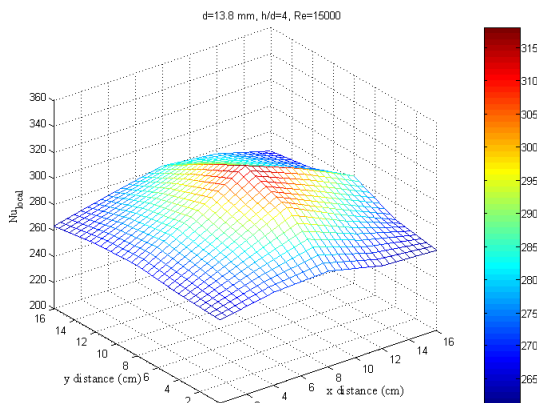


Fig. 3 Local Nu number distribution for $d = 13.8$ mm, $h/d = 4$, $Re = 15000$

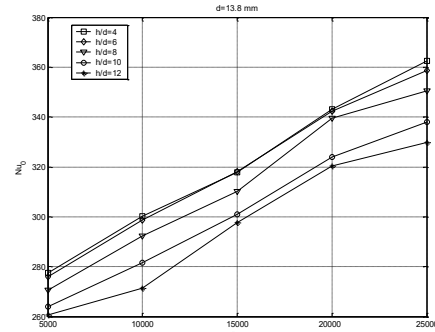


Fig. 6 Variation of stagnation point Nusselt number (Nu_0) with Re number for $d = 13.8$ mm flat circular nozzle.

The value of the average Nusselt number at the dimensionless distance $h/d = 4$ is also important. The

average Nusselt number (Nu_{avg}) was found to be $Nu_{avg}=256.9, 267, 278.6, 301.9$ and 305.7 in the range of Re number between 5000 and 25000, respectively. As can be seen from the values, the increase in the Re number increased the average Nusselt number.

Impingement Zone Flow Character

In this part of the study, mean velocity and turbulence intensity measurements of straight circular jets are presented graphically. The initial aim of the mean velocity and turbulence intensity measurements is to observe the flow dynamics in the flow region in the free jet state in the absence of impingement and then to determine the flow characteristics in the region close to the plate in the event of impingement. In particular, it was aimed to analyse the wall jet region and the impingement (or stall) region by placing the probe close to the plate during the jet impingement. However, the thickness of the probe cable and the thickness of the glass rods carrying the cable prevented the probe tip from fully contacting the plate (the distance between the probe and the plate is approximately 3.2 mm in all experiments). In this case, the wall jet region including the boundary layer thickness could not be analysed. The measurements taken were limited to measurements of the impingement zone close to the slab. Fig. 7 shows the coordinate axes and the measurement mechanism for both cases.

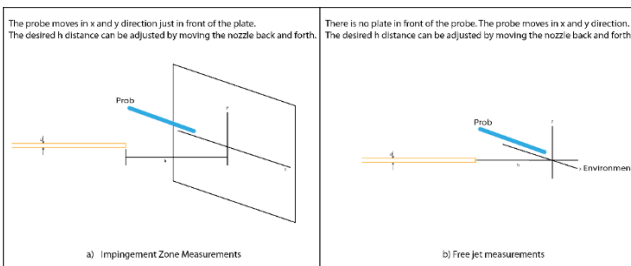


Fig. 7 Coordinate plane used in flow dynamics experiments

The most remarkable feature of free jets is the extremely unsteady nature of the flow. The stability of the jet flow is characterised by the Reynolds number, which is defined as the maximum velocity and flow width of the jet. When the Reynolds number has low values ($Re \approx 10-50$), periodic velocity variations are observed in the jet. These periodic variations weaken and disappear as the jet moves in the flow direction before turning into irregular turbulence. However, if the Reynolds number exceeds about 50, these periodic variations turn into irregular turbulent flow regime. The frequency of the periodic variation of the jet is found to be proportional to the square of the velocity.

Research has shown that in the absence of impingement, the flow fields of planar jets propagating in a stationary medium can be divided into three main regions. These regions are named as potential core (PC) region, characteristic distortion (CD) region and asymmetric distortion (AD) region [16-18]. The direction of the velocity profiles on the jet axis, depending on their propagation in the cross-section, was determined by analyses on the point axis.

Schlichting [21] and other researchers have suggested that the jet half-width varies proportional to $(h/d)^{2/3}$ and x

under laminar and turbulent flow conditions in planar jets, respectively. It was also stated that the centre line velocity varies proportional to $x^{-1/3}$ in laminar flow and $x^{-1/2}$ in turbulent jet flow. Schlichting [21] and other studies [1, 20] stated that the potential core region in circular free jets covers a distance of 12 times the jet outlet half width for turbulent flow, i.e. 6 times the jet diameter.

In the light of this theoretical information, the data obtained from experimental studies were evaluated. In the experiments, a circular jet with a diameter $d=13.8\text{mm}$ was used and the Reynolds number range was determined as $Re=5000-25000$. The graphs showing the free propagation of the jet in these ranges are presented in Figs. 8-13. These results are in agreement with the potential core and distortion regions defined in the theoretical literature. The experimental data confirm the behaviour of the flow in the turbulent regime and contribute to the characterisation of the jet propagation properties.

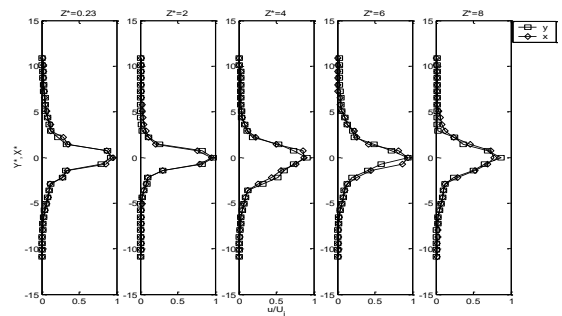


Fig. 8 Variation of average velocity with Z^* for $Re = 25000$ in a circular nozzle with $d = 13.8$ mm, $U_j = 5.5$ m/s

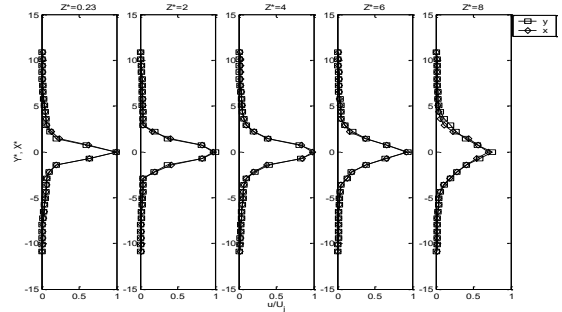


Fig. 9 Variation of average velocity with Z^* for $Re = 25000$ in a circular nozzle with $d = 13.8$ mm, $U_j = 11.35$ m/s

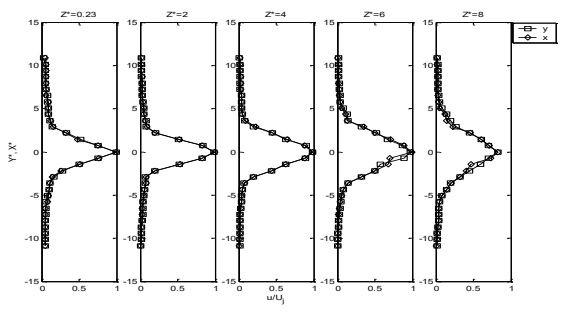


Fig. 10 Variation of average velocity with Z^* for $Re = 25000$ in a flat nozzle with $d = 13.8$ mm $U_j = 16.5$ m/s

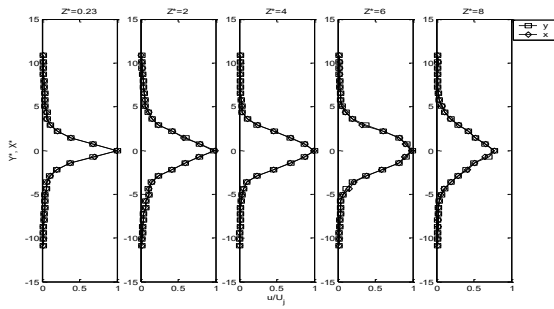


Fig. 11 Variation of average velocity with Z^* for $Re = 25000$ in a flat nozzle with $d = 13.8$ mm, $U_j = 22.5$ m/s

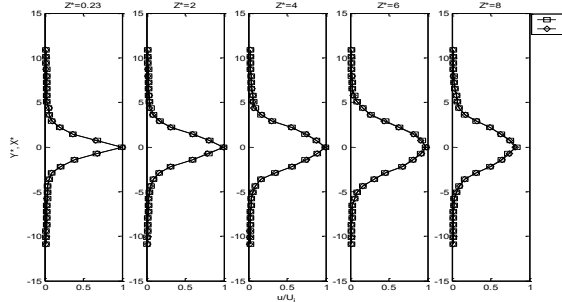


Fig. 12 Variation of average velocity with Z^* for $Re = 25000$ in a flat nozzle with $d = 13.8$ mm, $U_j = 27.5$ m/s

It can be seen from the figures that the centre line velocity remains approximately constant until $Z^* = h/d = 6$. When the current is further increased and reaches $Z^* = 8$, the centre line velocity decreases by about %22.19. This shows that there is a rapid deceleration in the circular jet after the potential core region.

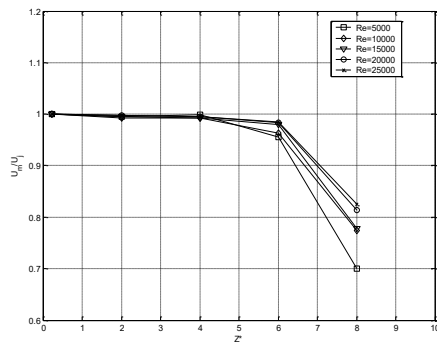


Fig. 13 Ratio of centre line velocity to jet outlet velocity for free jet for $d = 13.8$ mm

In Fig. 13, the variation of the centre line velocities with respect to each axial distance is also given for each Re number. As can be seen from the figure, the potential core region is very close to $Z^* = 6$. Another important feature of a circular jet stream is the classical bell curve shaped velocity profiles. Although it varies depending on the jet outlet nozzle and aspect ratio, a bell curve profile is seen in most jet streams. The difference between the highest value at the top of the curve and the value measured at the extreme point gives the dimensions of the transverse and longitudinal distribution of the velocity in the medium.

Turbulent Velocity

The turbulence intensity values generated during the propagation of a flat circular nozzle with a diameter of $d = 13.8$ mm into the stationary medium in the form of a free jet are dimensionless and shown in the graphs between Figs. 14-18. As in the previous section, the graphs are plotted according to the values of Re number in the range of 5000-25000.

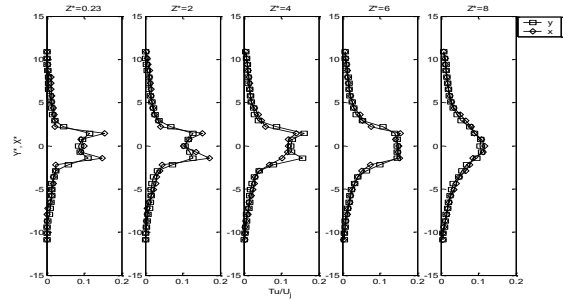


Fig. 14 Variation of turbulence intensity with Z^* for $Re = 5000$ in $d = 13.8$ mm flat nozzle $U_j = 5.5$ m/s

A key feature observed in turbulence intensity measurements is the saddle-backed profile, which appears when a jet with maximum centerline velocity exhibits sharp peaks near the center region. As noted in the theoretical section, these peaks may result from either the transition from laminar to turbulent boundary layer flow [19], or the formation of vortices in the shear stress region surrounding the jet [22, 23]. While researchers have highlighted both mechanisms, the primary concern in this study is their impact on heat transfer. The detailed causes and formation mechanisms of these peaks represent a separate area of investigation.

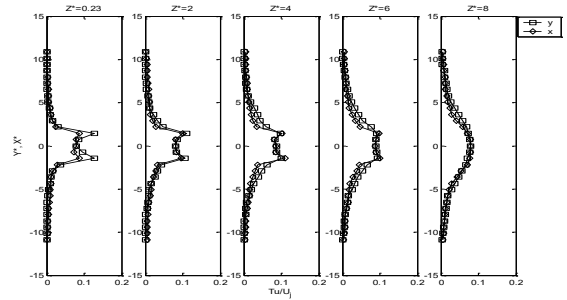


Fig. 15 Variation of turbulence intensity with Z^* for $Re = 10000$ in $d = 13.8$ mm diameter flat nozzle $U_j = 11.35$ m/s

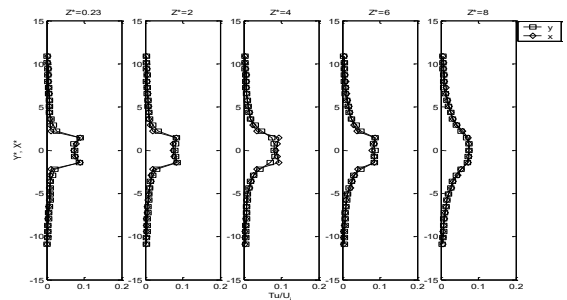


Fig. 16 Variation of turbulence intensity with Z^* for $Re = 15000$ in $d = 13.8$ mm diameter flat nozzle $U_j = 16.5$ m/s

In all graphs between Figs.14-18, it is observed that the turbulence intensity values first increase and then decrease with axial distance. The increasing part is up to $Z^*=6$ in all experiments. A slight decrease starts at $Z^*=8$. At Re number 5000, this increase is 23.99% from $Z^*=0.23$ to $Z^*=2$. There is an increase of 46.00% from $Z^*=0.23$ to $Z^*=4$, an increase of 69.01% from $Z^*=0.23$ to $Z^*=6$ and a decrease of 21.61% from $Z^*=0.23$ to $Z^*=8$. As it can be seen, while the turbulence intensity increases at high rates until $Z^*=6$, the percentage amount starts to decrease from $Z^*=8$.

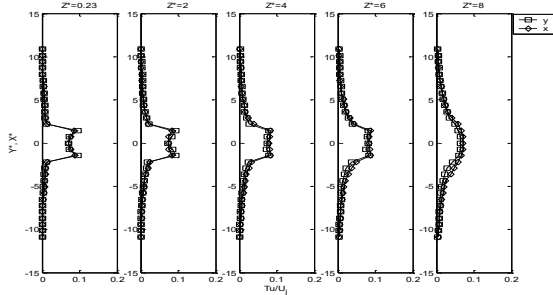


Fig. 17 Variation of turbulence intensity with Z^* for $Re=20000$ in $d=13.8$ mm diameter flat nozzle $U_j=22.5$ m/s

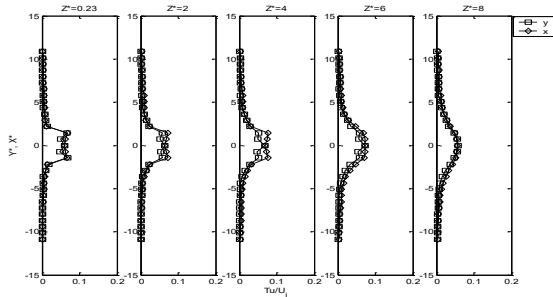


Fig. 18 Variation of turbulence intensity with Z^* for $Re=25000$ in $d=13.8$ mm diameter flat nozzle $U_j=27.5$ m/s

In the literature, the researchers who made turbulence intensity measurements in the free jet have shown the area where the turbulence velocity starts to decrease by mixing with the still air as a distance of 8-10 times the nozzle diameter. For example, in the experiments of Lee et al [24] with a 13 mm diameter flat circular tubular nozzle at Re numbers close to those in this study, it was observed that the turbulence intensity would start to decrease when $h/d=8$. In the nozzle with a diameter of $d=13.8$ mm tested in this study, the turbulence intensity values show an increase up to a distance of $6d$ and a tendency to decrease after this distance. Fig. 19 shows the turbulence intensity values measured from the centre line.

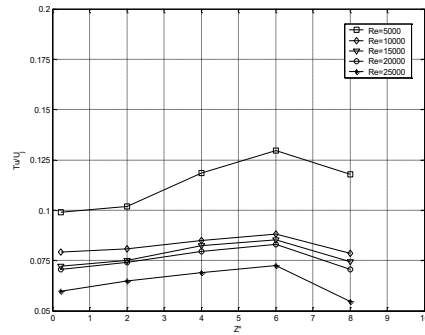


Fig. 19 Ratio of turbulence intensity to jet outlet velocity in case of free jet for $d=13.8$ mm

Distance Measurements Close To The Impingement Plate

Studies on the free-state flow dynamics of jet streams have been increasing with the developing technology so far. However, as mentioned in the introduction, there is a lack of studies on the impingement region. The theoretical analysis of the impingement region is quite difficult and there is not enough information in fluid mechanics in this part. Because, while it is possible to reach a solution for the problem related to the impingement flow in the two-dimensional continuous regime with the Navier-Stokes equations, it cannot be used because it cannot be defined in turbulent flow [1,25].

The hot-wire anemometer used in this study is a device that can take instantaneous measurements at a single point, but cannot be used to analyse the vectorial change of velocity. It is also clear that it cannot be sufficient for the investigation of a highly sensitive region containing boundary layer flow. Based on this fact, it was found more logical to investigate the effect of changing the distance between the nozzle and the plate in the area close to the impingement point rather than determining the details of the velocity and turbulence generated during the impingement. Secondly, the factor that led us to this choice can be explained as follows: When analysing the heat transfer during the impingement of the jet from the nozzle on the plate, it is important to see how the two parameters that seem to be effective on heat transfer, namely the change in the distance between the nozzle and the plate and the number Re , affect the velocity and turbulence. Thus, it was thought that it would be correct to examine how these two parameters, which provide a high rate of cooling during impingement, create a flow effect. Finally, the fact that such an investigation has not been widely reported in the literature is the third main factor in this choice.

The flow dynamics of fully developed circular jets, as described in the literature review, can be divided into four main regions: the free jet, the developing jet, the stall or impingement region and the wall jet. In the impingement region, the flow is influenced by the target surface and slows down and then accelerates, both vertically and horizontally, respectively. Tani and Komatsu [26] showed that this region can extend from the impingement surface to a distance of approximately twice the nozzle diameter ($L_{dz}= 2d$). Girald et al [27] reported that the height of the

distortion zone is 1.2 times the nozzle diameter. The effect of increasing or decreasing the distance between the nozzle and the plate on the impingement zone has not been analysed much in the literature so far.

Velocity and turbulence intensity values close to the plate were measured in both vertical and horizontal directions (Y^* , X^*). Measurements were taken at different nozzle-to-plate distances ($h/d=4, 6, 8, 10$ and 12). In 92 of the 100 experiments with straight circular jets, the deviations of the measured values in the X^* and Y^* axes at the top-bottom and right-left sides of the stagnation point are so small that they can be expressed in thousandths. The deviations observed in the remaining experiments are due to experimental errors. Although the quasi-symmetry condition was found to be met after the first experiments, the experiments were continued by taking measurements on both axes in order to determine the uncertainty analysis and to derive appropriate correlations. However, the results obtained in these experiments confirmed that measurements can only be taken from one of the X^* or Y^* axes in the flow dynamics tests of co-axial jets, which will be presented in the next section.

Average Speed Values

As the distance from the jet outlet increases, the momentum transfer between the jet and the environment leads to an expansion of the free boundary of the jet and a narrowing of the constant velocity core. Below the core, the velocity profile is not constant over the entire jet cross section and the peak velocity (at the midpoint) decreases with increasing distance from the nozzle outlet. As seen in Figs. 20-25, $u/U_j=1$ for all Re numbers at $h/d=4$ and $h/d=6$. More precisely, when the probe is 3.2 mm away from the plate, the velocity of the air jet impinged on the plate is measured equally until the distance between the nozzle and the plate is $6d$. This is the flow region where the surrounding fluid mixes with the jet and thus the jet velocity tends to decrease from the nozzle outlet. As the distance between the nozzle and the plate was increased ($8d, 10d$ and $12d$), the velocity measured at the geometrical centre of the plate also decreased. The geometrical centre point of the plate also coincides with the stagnation point as will be remembered in the heat transfer experiments. Apart from the distance between the nozzle and the plate, another parameter affecting the jet in the impingement zone is the Re number. In all experiments, the Re number was chosen in the range of 5000-25000 for comparison.

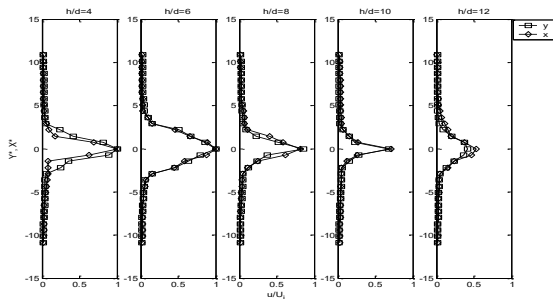


Fig. 20 Variation of average velocity with h/d when $d=13.8$ mm, $Re=5000$; $U_j=5.5$ m/s

In Fig.20, the velocity values measured in the impingement zone at various nozzle-plate distances at $Re=5000$ are given in dimensionless form. When $Re=5000$, the average velocity decreased by 85, 67 and 41% at $h/d=8, 10$ and 12 , respectively, compared to the jet outlet velocity when the distance between the nozzle-plate is outside the free jet in the vertical (Y^*). Similarly, in the horizontal (X^*), the reduction rates are 81, 71 and 53 percent. The area of influence of the jet is also at short distances at low values of Re number.

At Re 5000, the velocity measured at the geometrical centre point of the nozzle ($X^*=Y^*=0$) is equal to the jet outlet velocity until the nozzle-slab distance is six times the diameter. This area is the potential core region ($L_{pc}=6d$) and it is observed that the air velocity measured above the geometrical centre point decreases as one moves out of the potential core. This decrease is 18.08% at $h/d=8$ compared to $h/d=6$, 28.71% at $h/d=10$ compared to $h/d=6$ and 46.47% at $h/d=12$ compared to $h/d=6$. Figure (20) clearly shows that the velocity decreases significantly in both X^* and Y^* directions as it moves away from the centre point. These decreases are calculated as 98.9% at $h/d=4$, 98.76% at $h/d=6$, 97.89% at $h/d=8$, 97.64% at $h/d=10$ and finally 96.83% at $h/d=12$. As can be seen, as the nozzle plate distance increased, the reduction rates decreased. In other words, the values at the end are closer to the values at the midpoint. It is the expected characteristic of the jet that the current spreads over a wider area in a wider nozzle-plate range. Due to the small nozzle diameter, the reduction ratios are around 90%, which is quite high.

Fig. 21 shows the dimensionless velocity distribution when the jet outlet velocity is 11.35 m/s for Re number 10000. Increasing the Re number directly increases the velocity value at each measurement point. However, when the dimensionless velocity ratios are considered, u/U_j does not show a significant change with the increase of Re number. u/U_j dimensionless number rather shows how the jet is spread. It is seen that the velocity measured at the centre point remains constant until the distance $h/d=6$ at Re number 10000. Outside this region of constant velocity field, the velocities decrease as follows: at $h/d=8$, the dimensionless velocity value measured at the centre point decreases by 10.19% compared to $h/d=6$, at $h/d=10$ by %34.5 compared to $h/d=6$, and finally at $h/d=12$ by 49.92% compared to $h/d=6$.

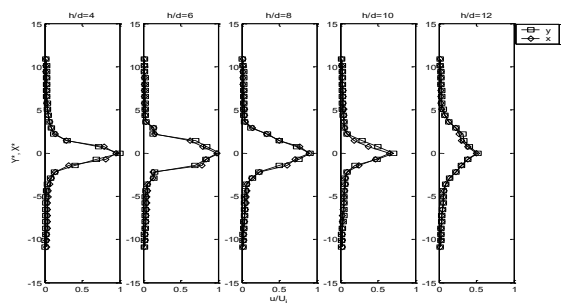


Fig. 21 Variation of average velocity with h/d when $d=13.8$ mm, $Re=10000$; $U_j=11.35$ m/s

Starting from the centre point -and it is worth reminding again that this point is the stagnation point on the plate- there is a significant decrease in the velocity value as we

move towards the endpoints of the X^* and Y^* axes. These decreases are 98.84% at $h/d=4$, 98.56% at $h/d=6$, 98% at $h/d=8$, 96.94% at $h/d=10$ and 96.29% at $h/d=12$.

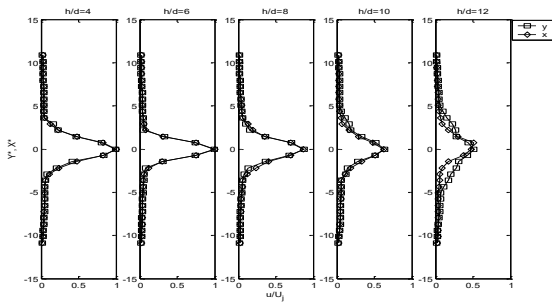


Fig. 22 Variation of average velocity with h/d when $d=13.8$ mm, $Re=15000$; $U_j=16.35$ m/s

In Fig. 22, the number of Re is increased to 15000. Increasing the Re number caused a decrease in the velocity outside the potential core. Namely: 13.202% decrease in dimensionless velocity ratio (u/U_j) at $h/d=8$ compared to $h/d=6$, 37.39% decrease at $h/d=10$ compared to $h/d=6$ and finally 51.68% decrease at $h/d=12$ compared to $h/d=6$. The decreases in the velocity ratio with moving away from the centre point are 98.11% at $h/d=4$, 98.15% at $h/d=6$, 97.36% at $h/d=8$, 96.6% at $h/d=10$ and finally 95.88% at $h/d=12$.

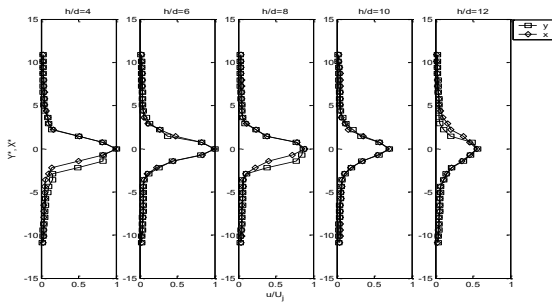


Fig. 23 Variation of average velocity with h/d when $d=13.8$ mm, $Re=20000$; $U_j=22.5$ m/s

Fig. 23 shows the velocity distributions in the impingement zone at 20000 values of Re . From the graph, it is possible to see how increasing the nozzle-plate distance changes the velocity value penetrating the stagnation point of the plate. However, if it is expressed in numbers; it is seen that the velocity outside the potential core is 11.10% at $h/d=8$, 30.16% at $h/d=10$ and 45.04% at $h/d=12$ compared to the velocity in the potential core region ($h/d=6$). In the range of $0 \leq x/d \leq 10$, high reductions in velocity were recorded. 97.76% at $h/d=4$, 97.92% at $h/d=6$, 96.34% at $h/d=8$, 96.6% at $h/d=10$ and 95.5% at $h/d=12$.

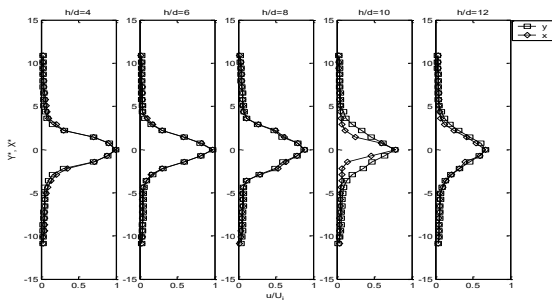


Fig. 24 Variation of average velocity with h/d when $d=13.8$ mm, $Re=25000$; $U_j=27.5$ m/s

At 25000, the maximum tested value of Re number, there is a decrease of 11.06% at $h/d=8$, 21.87% at $h/d=10$ and 33.06% at $h/d=12$ compared to $h/d=6$. Compared to the farthest measurement point from the stagnation point, there is a decrease of 97.47% at $h/d=4$, 97.55% at $h/d=6$, 97.71% at $h/d=8$, 96.34% at $h/d=10$ and finally 95.32% at $h/d=12$ (Fig. 24). One of the most important features seen in all Re number values given is that the velocity is at high values in a small area especially around the stagnation point and then shows a very rapid decrease. In fact, if we look at the percentage values calculated for all experiments; it is seen that there is a decrease of 95~98% between the stagnation point and the farthest x/d distance. The highest speed values are observed between $1.45 \leq x/d \leq 1.17$. The classical bell curve speed profile flattens at the tip and increases towards the edges as the h/d distance increases. The variation of the velocity values measured in front of the stagnation point according to the nozzle-plate distance is given in Fig. 25 separately according to X^* and Y^* axes.

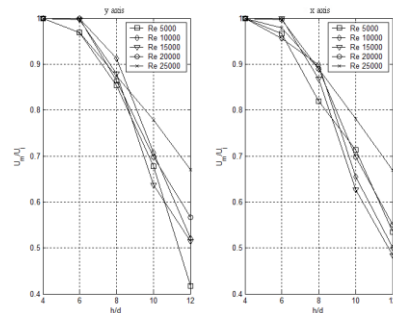


Fig. 25 Ratio of centreline velocity to jet outlet velocity at stagnation point for $d=13.8$ mm

Turbulence Intensity Measured in Front of the Plate

In the nozzle type with $d=13.8$ mm, it is observed that the turbulence intensity values measured in cases where the distance between the nozzle and the plate is short, peak values are observed near the stagnation point. In the absence of an impingement, peak values occur up to a maximum distance of $4d$ from the nozzle in the free jet position, but in the presence of an impingement, it can be seen that even the jet impinging at a distance of $6d$ in front of the plate makes second maximal. The presence of the plate may cause second and sometimes third peaks above the stagnation point.

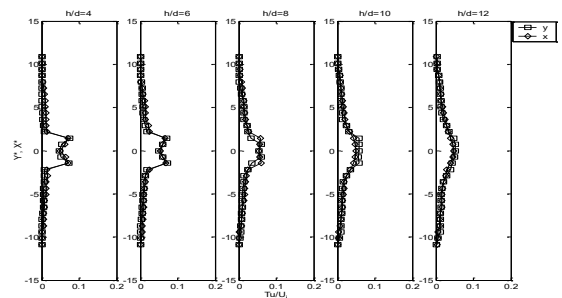


Fig. 26 Variation of turbulence intensity with h/d when $d=13.8$ mm, $Re=5000$; $U_j=5.5$ m/s

In Fig. 26, it is observed that increasing the distance of the nozzle hitting the plate increases the turbulence intensity value at the centre point of the plate up to a certain extent and then decreases it. From $h/d=4$ to $h/d=6$, the turbulence value increased by 7.76%. Between h/d 4 and 8, there is an increase of 9.77%. From $h/d=4$ to $h/d=10$, a slight increase of =3.64% was recorded. However, from $h/d=4$ to $h/d=12$, the turbulence intensity measured at the centre tends to decrease by 4.8%. This means that increasing the distance between the nozzle and the plate can increase the turbulence intensity value on the plate up to $h/d=10$. This is in agreement with the statement of Lee et al. [24] in their free jet and impingement turbulence values that ‘turbulence will increase up to a distance of 8-10d and then decrease’.

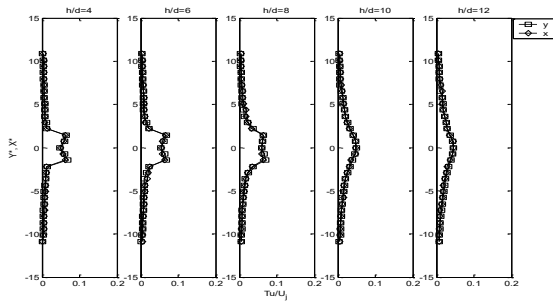


Fig. 27 Variation of turbulence intensity with h/d when $d=13.8$ mm, $Re=10000$; $U_j=11.35$ m/s

When the effect of increasing the nozzle-plate distance at Re number 10000 on the impingement event is analysed, when an evaluation similar to the above calculation is made, the following result is obtained: Compared to the closest nozzle distance $h/d=4$, the turbulence intensity increased by 10.51% on the plate at $h/d=6$ distance. Similarly, based on $h/d=4$, an increase of 18.37% at $h/d=8$, 5.61% at $h/d=10$ and a decrease of 9.63% at $h/d=12$ were observed (Fig. 27).

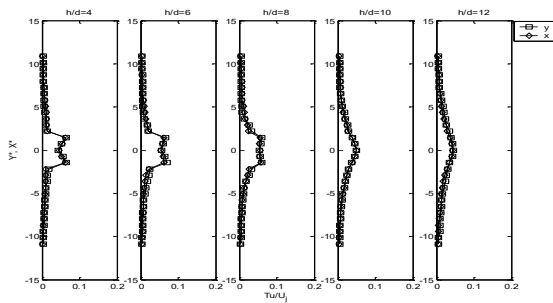


Fig. 28 Variation of turbulence intensity with h/d when $d=13.8$ mm, $Re=15000$; $U_j=16.5$ m/s

At the 15000 value of Re number shown in Fig. 28, the increase in $h/d=6$ compared to $h/d=4$ reaches a figure of 11.53%. The rate of increase in $h/d=8$ is 16.15%, 8.71% in $h/d=10$. $h/d=12$ shows a decrease of 4.77%.

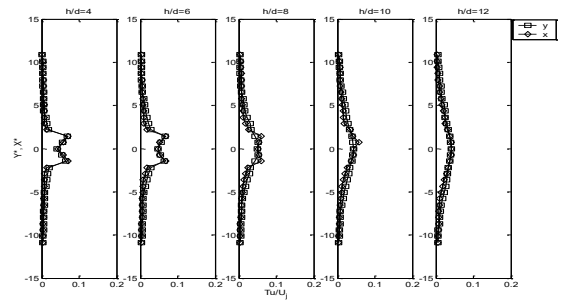


Fig. 29 Variation of turbulence intensity with h/d when $d=13.8$ mm, $Re=20000$; $U_j=22.5$ m/s

In Fig. 29, i.e. at $Re=20000$, the rates of increase between $h/d=6-10$ are calculated as 11.46%, 21.48%, 0.44% respectively compared to $h/d=4$. The rate of decrease at $h/d=12$ compared to $h/d=4$ is around 2.97%.

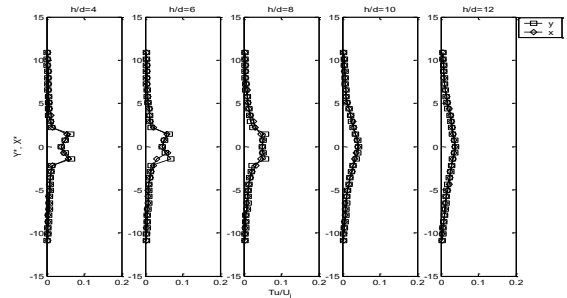


Fig. 29 Variation of turbulence intensity with h/d when $d=13.8$ mm, $Re=25000$; $U_j=27.5$ m/s

Finally, when the Re number was 25000 (Fig. 29), the effect of increasing the nozzle-sheet distance on the impingement was investigated; increasing h/d to 6 caused an increase of 15.16%, increasing $h/d=8$ caused an increase of 27.102%, and increasing $h/d=10$ caused an increase of 8.26% compared to the values at $h/d=4$. Subsequently, it was determined that there was a decrease of 3.78% at $h/d=12$. The % values obtained in the evaluations made so far do not show a complete systematic order. Looking at these values, it is difficult to emphasise whether increasing the number of Re is related to increasing the h/d distance. However, it would not be wrong to conclude that increasing the number of Re (even if there are deviations in between) has relatively increased the percentage increase rates. One of the general features of the turbulence curves plotted in Figs. 25-29 is that the turbulence measured in front of the impingement plate at distances $h/d>8$ is almost like a free jet turbulence profile. The only difference is that the values are higher here. However, the profiles are very similar. Finally, in figure (30), the variation of the turbulence values measured at the centre with respect to h/d and Re number is shown separately on the X^* and Y^* axes.

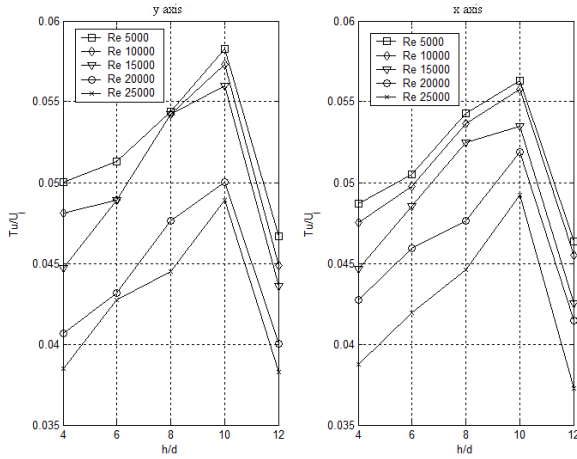


Fig. 30 Ratio of dimensionless turbulence intensity to jet outlet velocity measured at the stagnation point for $d=13.8$ mm

Conclusions

This study comprehensively analyzed the heat transfer and flow dynamics characteristics of a circular impinging jet under varying Reynolds numbers (5000–25000) and nozzle-to-plate distances ($h/d=2-10$). Using an aluminum nozzle with a diameter of 13.8mm, the experiments provided valuable insights into the relationship between jet parameters and thermal performance, highlighting the critical influence of Reynolds number and nozzle spacing on local and average Nusselt numbers. The findings emphasize the interplay between jet velocity, turbulence, and thermal boundary layer dynamics in determining heat transfer efficiency. The results revealed that increasing the Reynolds number significantly enhances heat transfer performance, with higher stagnation point (Nu_0) and average (Nu_{avg}) Nusselt numbers. Optimal performance was observed at intermediate nozzle-to-plate distances ($h/d \approx 4-6$), where turbulence intensity and momentum transfer were maximized. Beyond this range, heat transfer efficiency diminished due to the dissipation of jet momentum and turbulence. The thinning of the thermal boundary layer in the stagnation region was identified as a key factor driving enhanced heat transfer at the impingement point. The study also demonstrated that turbulence intensity plays a pivotal role, especially in the wall-jet region, where it contributes to greater mixing and momentum exchange.

A significant contribution of this research is the confirmation of theoretical models describing jet behavior, including the potential core, distortion regions, and decay characteristics. The experimental data validated the proportional relationships between Reynolds number, centerline velocity, and Nusselt number, providing strong agreement with established theoretical predictions. Additionally, preliminary tests indicated that conduction through the plate thickness accounted for less than 0.5% of the total heat transfer, affirming the reliability of the measurement approach.

This work not only enhances the understanding of impinging jet dynamics but also offers practical guidance for optimizing cooling systems in industrial and

engineering applications. Future research could expand upon these findings by exploring the effects of advanced nozzle geometries, pulsating jets, and nanofluids to further improve heat transfer efficiency. Furthermore, the integration of computational fluid dynamics (CFD) simulations with experimental analyses could provide a deeper understanding of complex flow and heat transfer mechanisms in impinging jet systems.

Nomenclature

Symbol	Description
h/d	Nozzle-to-plate distance ratio
h_{fg}	Latent heat of vaporization (J/kg)
ρ_v	Vapor density (kg/m ³)
U_j	Jet outlet velocity (m/s)
L_{dz}	Distortion zone height (times nozzle diameter, d)
L_{pc}	Potential core length (times nozzle diameter, d)
u/U_j	Dimensionless velocity ratio

Ethical Statement

The author declares that this document does not require ethics committee approval or any special permission.

Conflict of Interest

The author declares no conflict of interest

References

- [1] K. Jambunathan, E. Lai, M. A. Moss, and B. L. Button, "A Review of Heat Transfer Data for Single Circular Jet Impingement," *Int. J. Heat and Fluid Flow*, vol. 13, no. 2, pp. 106–115, 1992.
- [2] R. Gordon and J. C. Akfirat, "The Role of Turbulence in Determining the Heat Transfer Characteristics of Impinging Jets," *Int. J. Heat and Mass Transfer*, vol. 8, pp. 1261–1272, 1965.
- [3] E. U. Schlunder and V. Gnielinski, "Heat and Mass Transfer between Surfaces and Impinging Jets," *Chem. Ing. Tech.*, vol. 39, pp. 578–584, 1967.
- [4] C. Kistak, A. Taskiran, and N. Celik, "Experimental Analysis of Transient and Steady-State Heat Transfer from an Impinging Jet to a Moving Plate," *Heat and Mass Transfer*, vol. 60, pp. 1713–1729, 2024.
- [5] A. Taşkıran, C. Kistak, S. Kapan, N. Çelik, and İ. Dağtekin, "Numerical Analysis of Dual Slot Pulsating Nanofluid Impinging Jets", *DUJE*, vol. 15, no. 4, pp. 881–890, 2024.
- [6] G. Bai, G. Gong, and F. Zhao, "Multiple Thermal and Moisture Removals from the Moving Plate Opposite to the Impinging Slot Jet," *Appl. Therm. Eng.*, vol. 66, no. 1–2, pp. 252–265, 2014.

- [7] N. Celik and H. Eren, "Heat transfer due to impinging co-axial jets and the jets' fluid flow characteristics," *Exp. Therm. Fluid Sci.*, vol. 33, pp. 715–727, 2009.
- [8] K. Baghel et al., "Free Surface Planar Liquid Jet Impingement on a Moving Surface: Interfacial Flow and Heat Transfer Characteristics," *J. Mech. Sci. Technol.*, vol. 36, no. 11, pp. 5537–5549, 2022.
- [9] M. Rahimi and R. A. Soran, "Slot Jet Impingement Heat Transfer for the Cases of Moving Plate and Moving Nozzle," *J. Brazilian Soc. Mech. Sci. Eng.*, vol. 38, pp. 2651–2659, 2016.
- [10] J. Wang, X. Li, and S. A. Elmi, "Research on the Temperature and Thermal Stress of the Roll Quenching Process of Thin Plates," *Metals*, vol. 14, no. 1, p. 83, 2024.
- [11] Sparrow, E.M., and Gregg, J.L., A Boundary Layer Treatment of Laminar Film Condensation, *J. Heat Transfer*, 81, 13, 1959
- [12] Chen, M.M., An Analytical Study of Laminar Film Condensation Part I, *J. Heat Transfer*, 83, 48, 1961
- [13] Çelik, N., Optimum Lüle Tipinin Çarpan Jet Üzerindeki Etkilerinin İncelenmesi, Doktora Tezi, Fırat Üniv. Fen. Bil. Ens. Elazığ, 2006
- [14] Churchill, S.W. and Chu, H.H.S. (1975) Correlating Equations for Laminar and Turbulent Free Convection from a Vertical Plate. *International Journal of Heat and Mass Transfer*, 18, 1323-1329.
- [15] Kline, S.J., McClintock, F.A., Describing uncertainties in single-sample experiments, *Mechanical Engineering* 75, 3–8, 1953
- [16] Sfeir, A.A., "The Velocity and Temperature Fields of Rectangular Jet", *Int. J. Heat and Mass Transfer*, 19, 1289-1297, 1976.
- [17] Yevdjevich, V.M., "Diffusion of Slot Jets with Finite Length-Width Ratio", *Hydraulic Paper, Colarado State Univ.* 2, 1-40, 1966.
- [18] Sforza, P.M., Steiger, M.H., & Trentacoste, N., "Studies on Three Dimensional Viscous Jets", *AIAA J.* 4, 800-806, 1966.
- [19] Gauntner, J.W., Livingood, J.N.B., and Hrycak, P., "Survey of Literature on Flow Characteristics of Single Turbulent Jet Impinging on a Flat Plate", *NASA TN D-5652 NTIS N70-18963*, 1970.
- [20] Blevins, R.D., *Applied Fluid Dynamics Handbook*, Florida, 1992.
- [21] Schlichting, H., *Boundary Layer Theory*, McGraw Hill Co., New York, 1968.
- [22] Popiel, C.O., and Trass, O., "The Effect of Ordered Structure of Turbulence on Momentum, Heat and Mass Transfer of Impinging Round Jets, *Proc.7th Int. Heat Transfer Conf.*, Munchen, Germany, September 6-10, 6, 141-146, 1982.
- [23] Popiel, C.O., and Trass, O., "Visualization of a Free and Impinging Round Jet", *Exp. Thermal Fluid Science*, 4, 253-264, 1991.
- [24] Lee, D.H., Chung, Y.S. and Kim, D.S., "Turbulent Flow and Heat Transfer Measurements on a curved surface with a Fully Developed Round Impinging Jet", *Int. J. Heat and Fluid Flow*, 18, 160-169, 1997.
- [25] Can, O., "Elektronik Devrelerin Soğutulması ve Jet Püskürtmeli Soğutma Sistemlerinin Analizi" Yüksek Lisans Tezi, İTÜ Fen Bilimleri Enstitüsü, İstanbul, 1997.
- [26] Tani, I., and Komatsu, Y., "Impingement of a Round Jet on a Flat Surface", *Proc. of the Eleventh International Congress of Applied Mechanics*, (Editor H. Gortler), Springer-Verlag, New York, 672-676, 1966.
- [27] Giraldo, F., Chia C.J., and Trass, O., "Characterization of the Impingement Region in an Axisymmetric Turbulent Jet", *Ind. Eng. Chem. Fundam.* 16, 21-28, 1977.